Available online at www.sciencedirect.com
ScienceDirect
Journal of Photochemistry and Photobiology A: Chemistry 184 (2006) 147–154
Journal of Photochemistry and Photobiology A:Chemistry
www.elsevier.com/locate/jphotochem

Photooxidative *N*-de-methylation of crystal violet dye in aqueous nano-TiO_2 dispersions under visible light irradiation

Chiing-Chang Chen [a], Huan-Jung Fan [b], Chung-Yi Jang [b], Jeng-Lyan Jan [b], Hsiu-De Lin [b], Chung-Shin Lu [a,*]

[a] *Department of General Education, National Taichung Nursing College, Taichung 403, Taiwan*
[b] *Department of Environmental Engineering, Hungkuang University, No. 34, Chung-Chie Rd, Shalu, Taichung 433, Taiwan*

Received 3 September 2005; received in revised form 5 February 2006; accepted 10 April 2006
Available online 27 April 2006

Abstract

The photodegradation of dye pollutants under visible light irradiation in TiO_2 dispersions continues to draw considerable attention because of the improving effective utilization of cost free solar energy and its potential application to treating wastewater from textile and photographic industries. To get a better understanding of the mechanistic details of this TiO_2-assisted photodegradation of crystal violet dye (CV, *N*,*N*,*N*′,*N*′,*N*″,*N*″-hexamethylpararosaniline) with visible light irradiation, the intermediates of the process were identified and examined by HPLC–ESI-MS techniques in this research. The analytical results indicated nine intermediates, namely: *N*,*N*-dimethyl-*N*′,*N*′-dimethyl-*N*″-methylpararosaniline (DDMPR), *N*,*N*-dimethyl-*N*′-methyl-*N*″-methylpararosaniline (DMMPR), *N*,*N*-dimethyl-*N*′,*N*′-dimethylpararosaniline (DDPR), *N*-methyl-*N*′-methyl-*N*″-methylpararosaniline (MMMPR), *N*,*N*-dimethyl-*N*′-methylpararosaniline (DMPR), *N*-methyl-*N*′-methylpararosaniline (MMPR), *N*,*N*-dimethylpararosaniline (DPR), *N*-methylpararosaniline (MPR), and pararosaniline (PR). The experimental results indicated that the *N*-de-methylation degradation of CV dye took place in a stepwise manner to yield mono-, di-, tri-, tetra-, penta-, and hexa-de-methylated CV species. The possible degradation pathways were proposed and discussed in this research. The reaction mechanism of TiO_2/V proposed in this research would be useful for future application of the technology to the decoloration of dyes using solar energy.

Keywords: Crystal violet; Photodegradation; TiO_2; *N*-de-methylation

1. Introduction

The paper, leather, cosmetic, and food industries are major consumers for various types of triphenylmethane dyes [1–3]. Triphenylmethane dyes are used extensively in the textile industry for dyeing nylon, wool, cotton, and silk, as well as for coloring of oil, fats, waxes, varnishes, and plastics. Triphenylmethane dyes are used as staining agents in bacteriological and histopathological applications as well. The photocytotoxicity of triphenylmethane dyes based on the reactive oxygen species production is tested intensively using photodynamic therapy [4–7]. However, a great deal of concern has arisen regarding the thyroid peroxidase-catalyzed oxidation of the triphenylmethane class of dyes due to the generation of *N*-de-alkylated primary and secondary aromatic amines, which have structures similar to hazardous aromatic amine carcinogens [8].

It is reported that 10–20% of dyes are lost in wastewater as a result of inefficiency during the dyeing process [2]. The large amount of wastewater generated in textile manufacturing processes represents an increasing environmental danger due to the refractory carcinogenic nature of the dyes [9]. Therefore, dyestuffs generated from the textile and photographic industries are becoming a major source of environmental pollution. To de-pollute the dyeing wastewater, a number of methods – including chemical oxidation and reduction, chemical precipitation and flocculation, photolysis, adsorption, ion pair extraction, electrochemical treatment and advanced oxidation – have been investigated [10,11]. Advanced oxidation is one of promising technologies for the removal of dyes from contaminated wastewaters due to its high removal efficiency. This technology is mainly based on oxidative reactions with $HO^{\bullet}$ radical generated through various treatment methods such as O_3/UV, H_2O_2/UV,

* Corresponding author. Tel.: +886 4 22196973; fax: +886 4 22194990.
E-mail address: cslu6@ntcnc.edu.tw (C.-S. Lu).

1010-6030/$ – see front matter © 2006 Elsevier B.V. All rights reserved.
doi:10.1016/j.jphotochem.2006.04.008

H_2O_2/vis, O_3/H_2O_2/UV photolysis, photoassisted Fe^{3+}/H_2O_2, and TiO_2-mediated photocatalysis processes.

The TiO_2-mediated photocatalysis process has been successfully used to degrade dye pollutants for the past few years [12–18]. TiO_2 has the advantages of being photochemically stable, nontoxic, and low cost [19–21]. Kamat [22] reported that the mechanism of dye degradation in the presence of TiO_2 particles irradiated by visible light is not as same as the mechanism that occurs when particles are irradiated by UV light [22]. Possible reaction pathways for the self-sensitized photodegradation of dyes in aqueous TiO_2 dispersions illuminated by visible irradiation can be found elsewhere [23,24]. Under irradiation by visible light, dye radical cations ($dye^{\bullet+}$) and conduction band electrons (e_{cb}^-, usually taken to be surface Ti^{3+} ions) or electrons trapped in surface states were generated (Eqs. (1) and (2)). The electrons injected into the conduction band of the TiO_2 particles can either be scavenged by surface-adsorbed oxygen molecules to generate the superoxide radical anions $O_2^{\bullet-}$ or recombined with the $dye^{\bullet+}$ species (Eq. (3)).

$$\text{dye} + h^*\nu \rightarrow \text{dye}^* \quad (1)$$

$$\text{dye}^* + \text{TiO}_2 \rightarrow \text{TiO}_2(e_{cb}^-) + \text{dye}^{\bullet+} \quad (2)$$

$$\text{TiO}_2(e_{cb}^-)\,\text{dye}^{\bullet+} \rightarrow \text{dye} + \text{TiO}_2 \quad (3)$$

$$\text{dye} + {}^{\bullet}\text{OH} \rightarrow \text{degraded products} \quad (4)$$

$$\text{dye} + O_2^{\bullet-} \rightarrow \text{degraded products} \quad (5)$$

$$\text{dye}^{\bullet+} \rightarrow \text{degraded products} \quad (6)$$

$$\text{dye}^{\bullet+} + O_2^{\bullet-}\ (O_2 \text{ or } {}^{\bullet}\text{OH}) \rightarrow \text{degraded products} \quad (7)$$

After the initial photochemical steps (Eqs. (1) and (2)), a series of redox processes might involve the active radical species, such as $O_2^{\bullet-}$, $^{\bullet}$OH, and/or the radical cations, $dye^{\bullet+}$ (Eqs. (4)–(7)). These reactions would lead to photoassisted degradation of the dye and its intermediates.

Two competitive pathways have been proposed for the photodegradation of CV: (i) *N*-de-methylation of the chromophore skeleton and (ii) cleavage of the whole conjugated chromophore structure [25,26]. The *N*-de-methylation process was based on the presumption of the wavelength shift of maximal absorption of the dyes. However, the *N*-de-methylation intermediates of this dye have not been isolated or identified. Therefore, the mechanistic details of the process and cleavage of the whole conjugated chromophore structure remain to be investigated and confirmed.

Therefore, this research focused on identifying the *N*-de-methylation reaction intermediates of CV to investigate the mechanistic details of the *N*-de-methylation reaction of CV dye in the TiO_2/visible light process.

2. Experimental

2.1. Materials and reagents

Crystal violet (CV) was obtained from Tokyo Kasei Kogyo Co. and confirmed as a pure organic compound through HPLC analysis. Stock solutions containing 1 gL^{-1} of CV in aqueous solution were prepared, protected from light, and stored at 4 °C. The TiO_2 nanoparticle (P25, ca. 80% anatase, 20% rutile; particle size, ca. 20–30 nm; BET area, ca. 55 $m^2\,g^{-1}$) was supplied by Degussa Co.

Reagent-grade ammonium acetate, nitric acid, sodium hydroxide, and HPLC-grade methanol were purchased from Merck. De-ionized water was used throughout this study. The water was purified with a Milli-Q water ion-exchange system (Millipore Co.).

2.2. Instruments

A Waters ZQ LC/MS system with a Waters 1525 Binary HPLC pump, Waters 2996 Photodiode Array Detector, Waters 717plus Autosampler, and Waters micromass-ZQ4000 Detector were used to identify the reaction intermediates. The TiO_2/vis illumination experiment was conducted in a C-75 Chromato-Vue Cabinet of UVP with two 15-W visible lamps positioned on opposite sides of the cabinet interior.

2.3. Photodegradation experiments

An aqueous TiO_2 dispersion was prepared by adding 50 mg of TiO_2 powder into a 100 mL solution containing the CV at an appropriate concentration. The initial pH of the suspensions was adjusted by addition of either NaOH or HNO_3 solution to the desired value. Prior to irradiation, the dispersions were magnetically stirred in the dark for 30 min to ensure the adsorption/desorption equilibrium. At given irradiation time intervals, the dispersions were sampled (5 mL), centrifuged, and subsequently filtered through a Millipore filter (pore size, 0.22 μm) for analysis.

2.4. Procedures and analyses

The amount of residual dye at each irradiation cycle was determined by HPLC. The analysis of organic intermediates was accomplished by HPLC–ESI-MS after readjustment of chromatographic conditions done to make the mobile phases (Solvents A and B) compatible with the working conditions of mass spectrometer. Solvent A was 25 mM aqueous ammonium acetate buffer (pH 6.9) and solvent B was methanol. LC was carried out on an Atlantis™ dC18 column (250 mm × 4.6 mm i.d., dp = 5 μm). The mobile phase flow rate was 1.0 mL/min. A linear gradient was run as follows: $t = 0$, $A = 95$, $B = 5$; $t = 20$, $A = 50$, $B = 50$; $t = 35$–40, $A = 10$, $B = 90$; $t = 45$, $A = 95$, $B = 5$. The column effluent was introduced into the ESI source of the mass spectrometer. The quadruple mass spectrometer equipped an ESI interface with heated nebulizer probe at 350 °C was used with an ion source of 80 °C. ESI was carried out with the vaporizer at 350 °C and nitrogen as sheath (80 psi) and auxiliary (20 psi) gas to assist the preliminary nebulization and to initiate the ionization process. A discharge current of 5 μA was applied. Tube lens and capillary voltages were optimized for maximum response during perfusion of CV standard.

Blank experiments performed in flasks containing CV dye without addition of TiO_2 showed no appreciable decolorization

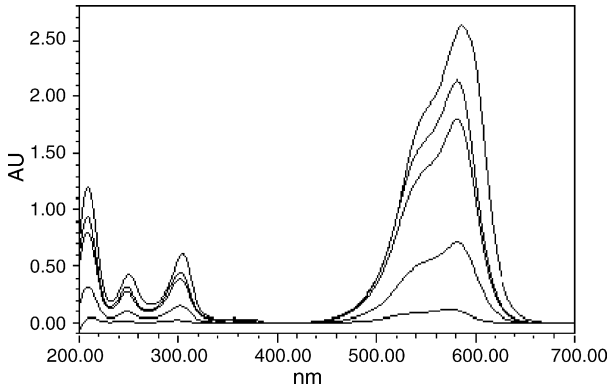

Fig. 1. The absorption spectra changes of CV in aqueous TiO_2 dispersions as a function of irradiation time. Spectra from top to bottom correspond to irradiation time of 16, 40, 64, 88, and 112 h, respectively (EV: 50 ppm, TiO_2: 50 mg/100 mL, and pH 6).

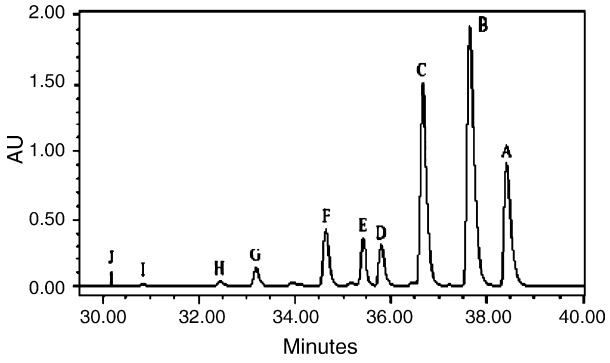

Fig. 2. HPLC chromatogram of the *N*-de-methylated intermediates at 80 h of irradiation, recorded at 580 nm.

of the dye. The stability of CV dye under visible irradiation was good as expected.

3. Results and discussion

The experimental results indicated that CV could be degraded efficiently in aqueous TiO_2 dispersions by visible light irradiation (Fig. 1). The concentration of dye was decreased with time. The degradation of CV at the end of 112 h irradiation time was about 92%. The characteristic wavelengths shifted slightly from 588.3 to 573.7 nm with time as well. This result indicated the possible formation of a series of *N*-de-methylated intermediates. The reaction intermediates in the above reactions were examined by HPLC using a photodiode array detector and ESI mass spectrometry. Ten components (A–J) were observed and identified. Results of HPLC chromatograms, UV–vis spectra, and HPLC–ESI mass spectra are summarized in Table 1.

The reaction intermediates of TiO_2/vis reaction are shown in Fig. 2. Peak A is CV dye, and peaks B–J are reaction intermediates. The absorption spectra of each intermediate in the visible spectral region are measured and depicted in Fig. 3. The absorption spectral bands shift hypsochromically from 588.3 nm (Fig. 3, Spectrum A) to 543.2 nm (Fig. 3, Spectrum J). This hypsochromic shift of the absorption band was possible due to the formation of a series of *N*-de-methylated intermediates in a stepwise manner. For example, λ_{max} of CV, DDMPR, DMMPR, DDPR, MMMPR, DMPR, MMPR, DPR, MPR, and PR are 588.3, 581.0, 579.8, 573.7, 570.0, 566.3, 566.3, 561.5, 554.1, and 543.2 nm, respectively. This result is in agreement with the results presented in Fig. 1. Similar phenomena were reported for the photodegradation of sulforhodamine-B [12] and rhodamine-B [24] under the visible irradiation. Saquib and Muneer [25] studied the RhB/CdS system and stated that the electron from the singlet excited state $^1RhB^*$ to CdS particles came from the nitrogen atoms [25]. Therefore, the wavelength shift depicted in Fig. 3 might have been caused by the *N*-de-methylation of CV, which was due to the reaction between active oxygen species and the *N*,*N*-dimethyl group of the dye.

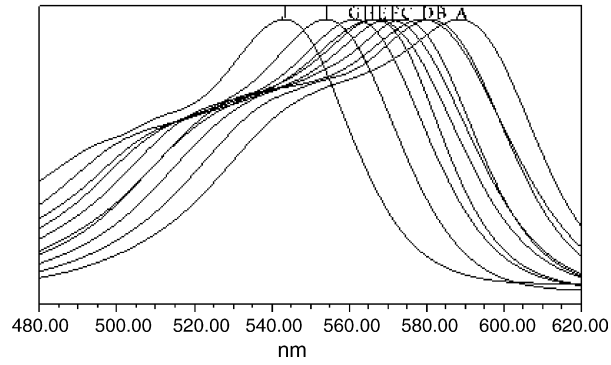

Fig. 3. Absorption spectra of *N*-de-methylated intermediates formed during the photodegradation of CV. Spectra were recorded using the photodiode array detector.

Table 1
The *N*-de-methylation intermediates of CV by TiO_2/vis process

HPLC peaks	De-methylation intermediates	Abbreviation	ESI-MS peaks	Absorption maximum (nm)
A	*N*,*N*,*N*′,*N*′,*N*″,*N*″-hexamethyl pararosaniline	CV	372.12	588.3
B	*N*,*N*-dimethyl-*N*′,*N*′-dimethyl-*N*″-methyl pararosaniline	DDMPR	358.20	581.0
C	*N*,*N*-dimethyl-*N*′-methyl-*N*″-methyl pararosaniline	DMMPR	344.21	573.7
D	*N*,*N*-dimethyl-*N*′,*N*′-dimethyl pararosaniline	DDPR	344.15	579.8
E	*N*-methyl-*N*′-methyl-*N*″-methyl pararosaniline	MMMPR	330.16	566.3
F	*N*,*N*-dimethyl-*N*′-methylpararosaniline	DMPR	330.16	570.0
G	*N*-methyl-*N*′-methylpararosaniline	MMPR	316.24	561.5
H	*N*,*N*-dimethylpararosaniline	DPR	316.11	566.3
I	*N*-methylpararosaniline	MPR	302.13	554.1
J	pararosaniline	PR	288.07	543.2

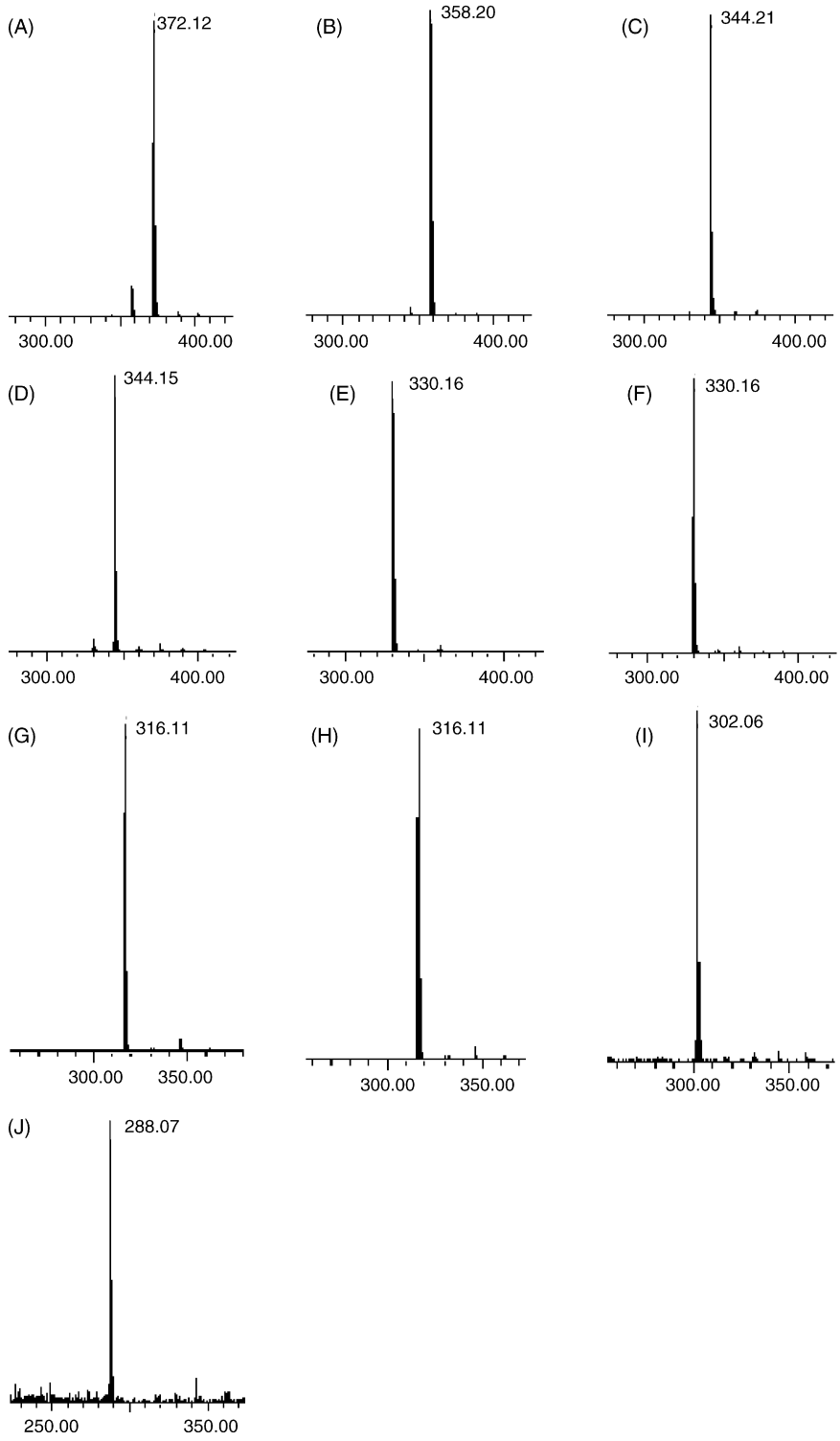

Fig. 4. (A–J) ESI mass spectra of the *N*-de-methylated intermediates formed during the photodegradation of the CV dye after they were separated by HPLC method.

As shown in Fig. 4, mass spectral analysis confirmed that the components A ($m/z = 372.12$), B ($m/z = 358.20$), C ($m/z = 344.21$), D ($m/z = 344.15$), E ($m/z = 330.16$), F ($m/z = 330.16$), G ($m/z = 316.11$), H ($m/z = 316.11$), I ($m/z = 302.06$), and J ($m/z = 288.07$) are CV, DDMPR, DMMPR, DDPR, MMMPR, DMPR, MMPR, DPR, MPR, and PR, respectively. CV dye has dimethyl groups on three sides. DDMPR (Fig. 5, compound **B**) is obtained by the removal of one methyl group from the CV molecule. DMMPR, DDPR, MMMPR, DMPR, MMPR, and DPR correspond to three pairs of isomeric molecules with two to four less methyl groups than CV as shown in Fig. 5 compounds **C**–**H**. DMMPR (Fig. 5, compound **C**), is formed by removal of a methyl group from two different sides of the CV molecule while the other

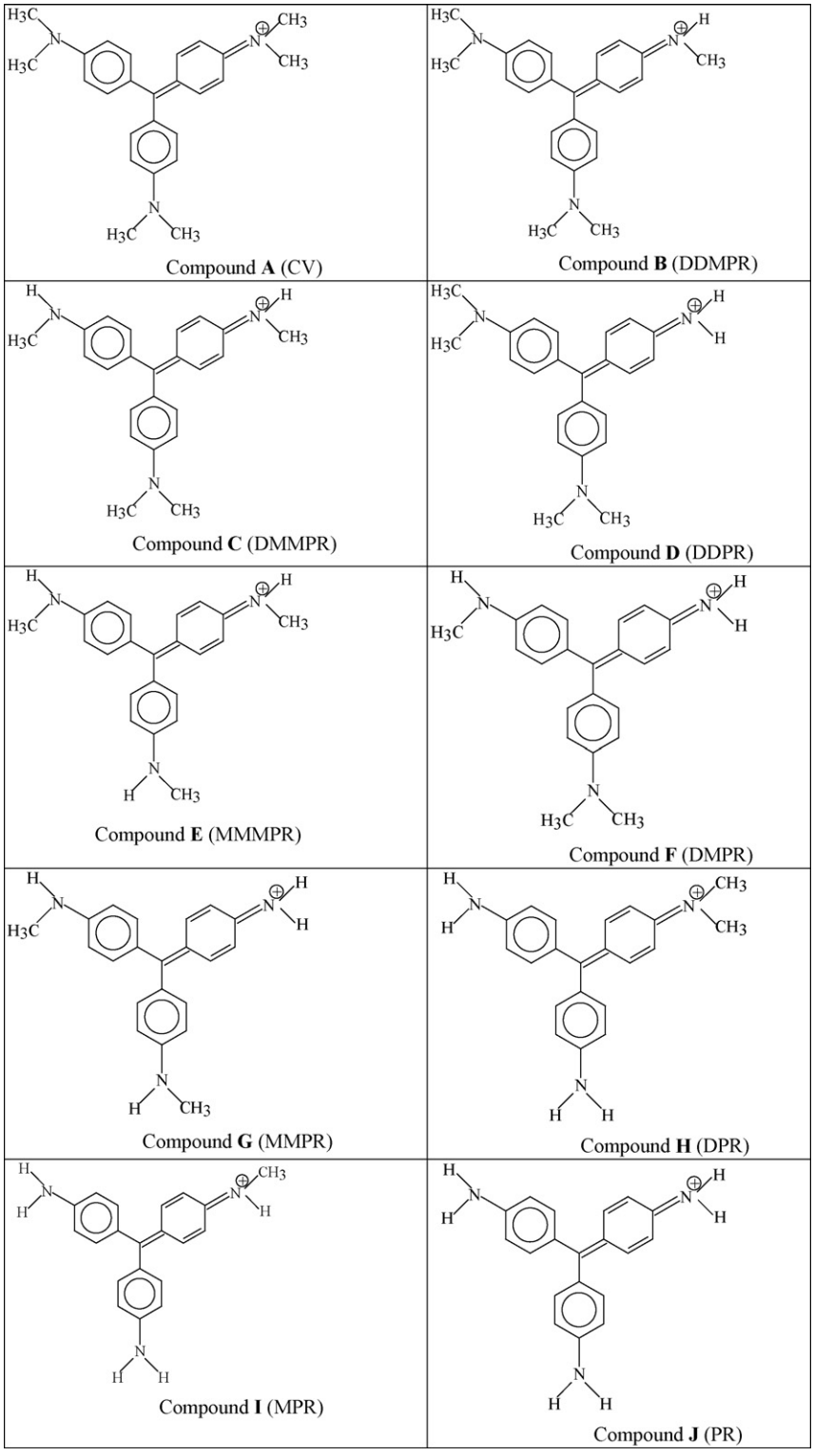

Fig. 5. Chemical structure of the *N*-de-methylated intermediates.

corresponding isomer in this pair, DDPR (Fig. 5, compound **D**), is produced by the removal of two methyl groups from the same side of the CV structure. In the second pair of isomers, MMMPR (Fig. 5, compound **E**), is formed by the removal of three methyl groups from each side of the CV molecule while the other isomer in this pair, DMPR (Fig. 5, compound **F**), is produced by removing two methyl groups from one side of the CV structure while one more was removed from the other side. In the third pair of isomers, MMPR (Fig. 5, compound **G**), is produced removing two methyl groups from one side of the CV structure and one for each of the rest of its two sides. The other isomer in this pair, DPR (Fig. 5, compound **H**), is formed

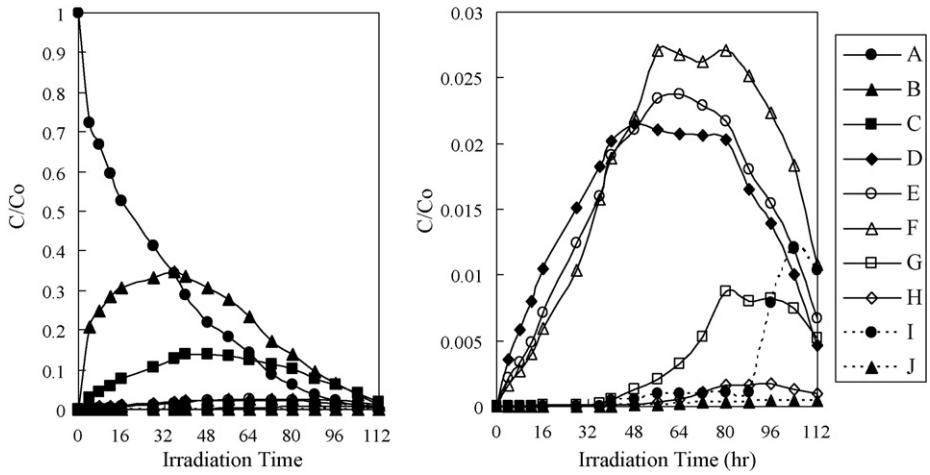

Fig. 6. Variations in the relative distribution of the *N*-de-methylated products obtained from the photodegradation of CV as a function of irradiation time.

removing two methyl groups from two different sides of the CV molecule. Compounds **I** (MPR) and **J** (PR) have one and zero methyl groups, respectively.

Considering that the polarity of the DDPR, DMPR, and DPR species exceeds that of the DMMPR, MMMPR, and MMPR intermediates, we expected the latter to be eluted after the DDPR, DMPR and DPR species. Additionally, to the extent that two *N*-methyl groups are stronger auxochromic moieties than are *N*,*N*-dimethyl or amino groups, the maximal absorption of the DDPR, DMPR and DPR intermediates was anticipated to occur at wavelengths shorter than the band position of the DMMPR, MMMPR, and MMPR species. Similar phenomena were reported for the photodegradation of sulforhodamine-B [12] under visible irradiation as well. The following results shown in Fig. 6 and the proposed mechanism support this argument.

The distributions of all of the *N*-de-methylated intermediates with irradiation time are illustrated in Fig. 6. To minimize errors, the relative intensities of each intermediate were recorded at the maximum absorption wavelength of each intermediate. The quantitative determination of all of the photogenerated intermediates was unfortunately not achieved, due to unavailability of the reference standards and appropriate molar extinction coefficients of these intermediates. The distributions of all of the *N*-de-methylated intermediates are intensities relative to the initial concentration of CV. Nonetheless, the changes in the distribution of each intermediate were observed during the photodegradation of CV as shown in Fig. 6.

Serpone et al. [24] suggested that *N*-de-ethylation was caused by the reaction of active oxygen species on the *N*-ethyl groups. Under UV irradiation, most of the $^{\bullet}OH$ is generated directly from the reaction between the electron holes and surface-adsorbed H_2O or OH^- on TiO_2 surfaces. However, the main pathway for the formation of reactive oxygen species under visible irradiation is through the reduction of O_2 by the conduction band electron.

Serpone and co-workers [24] stated that the generation of active oxygen species was determined by the spin-trap electron resonance techniques (ESR). The relative intensities of the superoxide radical anions, $O_2^{\bullet -}$, and hydroxyl radicals, $^{\bullet}OH$, during the visible irradiation at 532 nm (Nd:YAG laser) in the presence and absence of I^- ions have been reported. Although the hydroxyl radical was detected as DMPO–$^{\bullet}OH$ adduct in the ESR measurements, it is not the principal or sole species that leads to photooxidation of CV in the presence TiO_2 under visible irradiation. This was confirmed by control experiments [12,24]. In this study, since the probability for the formation of $^{\bullet}OH$ is much less than that of $O_2^{\bullet -}$, the *N*-de-methylation of the CV dye would occur mostly by the attack of the $O_2^{\bullet -}$ species. The $O_2^{\bullet -}$ species are excellent nucleophilic reagents for the *N*-methyl portion of CV.

3.1. Photoreaction pathways

Under visible light illumination, the semiconductor is not excited as its absorption threshold is 385 nm; only the chemisorbed CV is excited at wavelengths longer than 470 nm to produce singlet and triplet states (denoted here simply as CV^*_{ads}). Subsequently, CV^*_{ads} injects an electron into the conduction band (or to some surface state) of the semiconductor with CV being converted to the radical cation $CV^{\bullet +}$. In turn, the injected electron on the TiO_2 particle, TiO_2 (e^-), reacts with adsorbed oxidants, usually O_2, to produce reactive oxygen radicals (Eqs. (1)–(7)). Oxygen plays an additional important role here: in scavenging the electron, it suppresses recombination (back electron transfer) between $CV^{\bullet +}$ and e^-. The radical cation, $CV^{\bullet +}$, ultimately reacts with reactive oxygen radicals and/or molecular oxygen to yield intermediate products or other radical species, which, if secondary radical processes occurred, might lead to mineralization [27,28].

There are two possible major competitive reaction pathways for the generation of intermediates: (1) reaction with *N*,*N*-dimethyl groups and (2) reaction with *N*-methyl groups. Considering that the *N*,*N*-dimethyl groups of DDPR, DMPR and DPR are bulkier than those of the *N*-methyl groups of DMMPR, MMMPR, and MMPR molecules, respectively, nucleophilic attack by $O_2^{\bullet -}$ on the *N*-methyl groups should be favored over that on the *N*,*N*-dimethyl groups. However, considering that the attack probability on two *N*,*N*-dimethyl groups of DDPR is

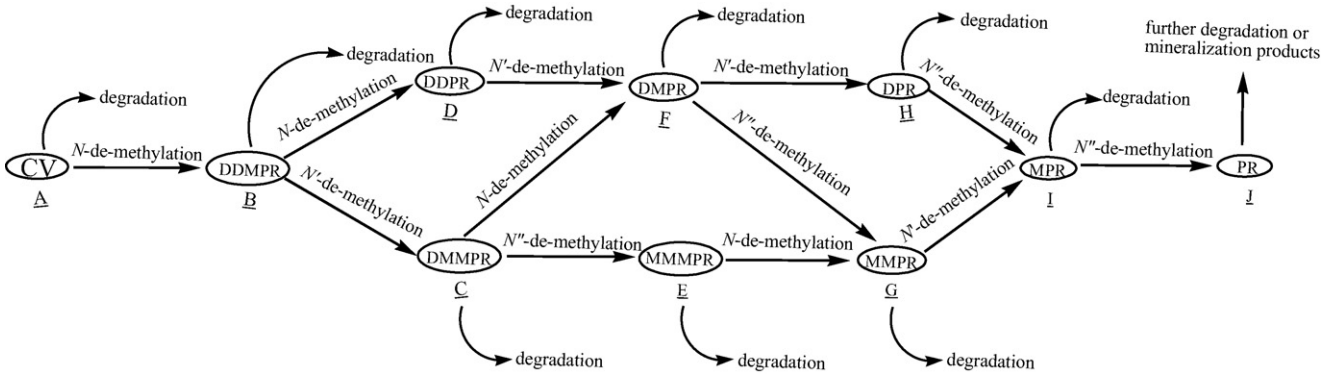

Fig. 7. Proposed *N*-de-methylation mechanism of crystal violet under visible light irradiation in aqueous TiO_2 dispersions followed by the identification of several intermediates by HPLC–ESI mass spectral techniques.

higher than that on one *N*-methyl group in DDMPR molecules, nucleophilic attack by $O_2^{\bullet -}$ on the *N*,*N*-dimethyl group should be favored over that on the *N*-methyl group.

The *N*-di-de-methylated intermediates (DMMPR [Fig. 6, C] and DDPR [Fig. 6, D]) reached their maximum concentrations at the same time (48 h irradiation time). This result indicated that both competitive pathways are significant.

The *N*-tri-de-methylated intermediates (MMMPR [Fig. 6, E] and DMPR [Fig. 6, F]) are observed in Fig. 6 as well. MMMPR reached its maximum concentration at 56 h. However, DMPR reached the maximum concentrations at both 56 and 80 h. DMPR was produced through the reaction of nucleophilic reagent on the *N*-methyl group of DMMPR and the *N*,*N*-dimethyl group of DDPR, respectively, as illustrated in Fig. 7. This could be the reason the DMPR had two maximum concentrations.

The *N*-tetra-de-methylated intermediates are MMPR (Fig. 6, G) and DPR (Fig. 6, H). MMPR reached the maximum concentration around 80 and 96 h into the irradiation period, and these two peaks correspond to the reaction of nucleophilic reagent on the *N*-methyl group of MMMPR and the *N*,*N*-dimethyl group of DMPR, respectively, as shown in Fig. 7. DPR had two maximum concentrations at 80 and 96 h as well. They were generated through the *N*-de-methylation of DMPR, which also had two major concentration peaks.

There was one *N*-penta-de-methylated intermediate (MPR, Fig. 6, curve I). MPR reached its maximum concentration after a 104-h irradiation period. It was a product of the nucleophilic reagent attack on the *N*-methyl group of MMPR and the *N*,*N*-dimethyl group of DPR.

PR (Fig. 6, curve J) is an *N*-hexa-de-methylated intermediate and reached its maximum concentration at 112 h irradiation time.

The successive appearance of the maximal quantity of these intermediates indicated that the *N*-de-methylation of CV is a stepwise photochemical process. For example, the first product (DDMPR) of *N*-de-methylation reached its maximum concentration after a 36-h irradiation time (Fig. 6, curve B) while the maximum of the final *N*-de-methylated product (PR) appeared after irradiating for 112 h (Fig. 6, curve J). The chromophoric species (CV) were slowly reduced with time (Fig. 6, curve A). This indicates that the *N*-de-methylation process predominates and the cleavage of the conjugated structure occurs at a somewhat slower rate until all six methyl groups are removed.

3.2. Reaction mechanisms

Examination of Figs. 1 and 2 and temporal behavior of Fig. 6 suggests that CV is *N*-de-methylated in a stepwise manner (i.e., methyl groups are removed one by one as confirmed by the gradual peak wavelength shifts toward the blue region). The hypsochromic shift process was the *N*-de-methylation process [25]. Therefore, during the initial period of the photodegradation of CV, *N*-de-methylation was a dominating mechanism, and cleavage of the CV chromophore ring structure was not the significant step.

According to the literature, the oxidative *N*-de-alkylation processes were preceded by formation of nitrogen-centered radical [26,29], and destruction of dye chromophore structures was preceded by generation of carbon-centered radical [30–32]. Both reaction pathways might be important in this research. Electron injection from the dye to the conduction band of TiO_2 yields dye cation radical, and this was confirmed by Liu [33] through determination of the nature of the HOMO orbital of the excited dye ($^{1,3}dye^*$) [33]. After this step, the cation radical ($dye^{\bullet +}$) can undergo hydrolysis and/or a deprotonation reaction.

Base on these experimental results, reaction pathways of *N*-de-methylation of CV are proposed and depicted in Fig. 7. Nucleophilic attack by $O_2^{\bullet -}$ on the *N*-methyl groups should be favored over that on the *N*,*N*-dimethyl groups. Considering, however, that the attack probability on two *N*,*N*-dimethyl groups of DDPR is higher than that of one *N*-methyl group in DDMPR molecules, nucleophilic attack by $O_2^{\bullet -}$ on the *N*,*N*-dimethyl group should be favored over that on the *N*-methyl group. This result indicated that both competitive pathways are significant. The *N*-tri-de-methylated intermediates MMMPR and DMPR are observed in Fig. 7 as well. MMMPR was produced through the reaction of nucleophilic reagent with the *N*,*N*-dimethyl group of DMMPR. DMPR was produced through the reaction of nucleophilic reagent with the *N*-methyl group of DMMPR and the *N*,*N*-dimethyl group of DDPR. The *N*-tetra-de-methylated intermediates are MMPR and DPR. MMPR was produced through the reaction of nucleophilic reagent with the *N*-methyl group

of MMMPR and the *N*,*N*-dimethyl group of DMPR. DPR were generated through *N*-de-methylation of DMPR. There was one *N*-penta-de-methylated intermediate (MPR), a product of the nucleophilic reagent attack on the *N*-methyl group of MMPR or the *N*,*N*-dimethyl group of DPR. PR is *N*-hexa-de-methylated intermediate (PR) generated through the *N*-de-methylation of DMPR.

In the CV/TiO_2, system, the dye molecule was adsorbed onto the TiO_2 surface through the positively charged dimethylamine function of dye. An electron was injected from the TiO_2 particle surface to the adsorbed dye. The adsorbed dye was hydrolyzed (or deprotonated) to yield a nitrogen-centered radical, which was subsequently attacked by molecular oxygen. The *N*-de-methylation of CV was the result of these reactions. The mono-de-methylated dye, PPR, could be excited by processes (electron injection, hydrolysis/deprotonation, and oxygen attack) described above or by visible light to yield a di-de-methylated dye derivative (DDPR and DMMPR). The *N*-de-methylation process as described above continued until formation of the completely *N*-de-methylated dye, PR. When *N*-de-methylation intermediates of CV were excited by visible light, the subsequent transformation of the carbon-centered cationic radicals generated further degradation or mineralization products.

4. Conclusion

CV could be successfully decolorized and degraded by TiO_2 at room temperature under visible irradiation. Both *N*-de-methylation and direct degradation of CV took place in presence of TiO_2 particles. The *N*-de-methylation process predominates during the initial irradiation period, and the *N*-de-methylated intermediates were confirmed by HPLC–ESI-MS and UV–vis spectra in this research for the first time. The successive appearance of the maximal quantity of each intermediate indicates that the *N*-de-methylation of CV was a stepwise photochemical process. The *N*-de-methylation process continues until formation of the completely *N*-de-methylated dye, PR. Experimental results indicated that the methyl groups were removed one at a time and confirmed by the gradual peak wavelength shifts toward the blue region. The reaction mechanisms of CV dye in the TiO_2/vis system were proposed and discussed in this research.

References

[1] Triarylmethane and diarylmethane dyes, in: Ullmann's Encyclopedia of Industrial Chemistry. Part A27, sixth ed., Wiley–VCH, New York, 2001.
[2] H. Zollinger, In Color Chemistry: Syntheses, Properties, and Applications of Organic Dyes and Pigments, second ed., VCH, Weinheim, 1991.
[3] R.L. Feller, Accelerated aging. Photochemical and thermal aspects, J. Paul Getty Trust (1994).
[4] A.C. Bhasikuttan, A.V. Sapre, L.V. Shastri, J. Photochem. Photobiol. A: Chem. 150 (2002) 59–66.
[5] M.S. Baptista, G.L. Indig, J. Phys. Chem. B 102 (1998) 4678–4688.
[6] R. Bonnett, G. Martinez, Tetrahedron 57 (2001) 9513–9547.
[7] A.J. Kowaltowski, J. Turin, G.L. Indig, J. Bioenerg. Biomember. 31 (1999) 581–590.
[8] B.P. Cho, T. Yang, L.R. Blankenship, J.D. Moody, M. Churchwell, F.A. Bebland, S.J. Culp, Chem. Res. Toxicol. 16 (2003) 285–294.
[9] A. Reife, Dyes environmental chemistry, in: Kirk (Ed.), Othmer Encyclopedia of Chemical Technology, vol. 8, fourth ed., John Wiley & Sons, Inc., New York, 1993, pp. 753–784.
[10] W. Azmi, R.K. Sani, U.C. Banerjee, Enzyme Microb. Technol. 22 (1998) 185–191.
[11] R.Y. Peng, H.J. Fan, Dyes Pigments 67 (2005) 153–159.
[12] C.C. Chen, W. Zhao, J.G. Li, J.C. Zhao, H. Hidaka, N. Serpone, Environ. Sci. Technol. 36 (2002) 3604–3611.
[13] H. Měšťánková, J. Krýsa, J. Jirkovský, G. Mailhot, M. Bolte, Appl. Catal. B: Environ. 58 (2005) 185–191.
[14] R. Asahi, T. Morikawa, T. Ohwaki, K. Aoki, Y. Taga, Science 293 (2001) 269–271.
[15] M. Karkmaz, E. Puzenat, C. Guillard, J.M. Herrmann, Appl. Catal. B: Environ. 51 (2004) 183–194.
[16] H. Kyung, J. Lee, W. Choi, Environ. Sci. Technol. 39 (2005) 2376–2382.
[17] H. Hidaka, H. Honjo, S. Horikoshi, N. Serpone, New J. Chem. 27 (2003) 1371–1376.
[18] P. Lu, F. Wu, N.S. Deng, Appl. Catal. B: Environ. 53 (2004) 87–93.
[19] A.L. Linsebigler, G.Q. Lu, J.T. Yates Jr., Chem. Rev. 95 (1995) 735–758.
[20] M.R. Hoffman, S.T. Martin, W. Choi, W. Bahnemann, Chem. Rev. 95 (1995) 69–96.
[21] C.S. Turchi, D.F. Ollis, J. Catal. 122 (1990) 178–192.
[22] P.V. Kamat, Langmuir 6 (1990) 512–513.
[23] T. Watanabe, T. Takizawa, K. Honda, J. Phys. Chem. 81 (1977) 1845–1851.
[24] T. Wu, G. Liu, J. Zhao, H. Hidaka, N. Serpone, J. Phys. Chem. B 102 (1998) 5845–5851.
[25] M. Saquib, M. Muneer, Dyes Pigments 56 (2003) 37–49.
[26] B.L. Laube, M.R. Asirvatham, C.K. Mann, J. Org. Chem. 42 (1977) 670–674.
[27] J. Zhao, T. Wu, K. Wu, K. Oikawa, H. Hidaka, N. Serpone, Sci. Technol. 32 (1998) 2394–2400.
[28] R.W. Matthews, Water Res. 25 (1991) 1169–1176.
[29] F.C. Shaefer, W.D. Zimmermann, J. Org. Chem. 35 (1970) 2165–2174.
[30] X. Li, G. Liu, J. Zhao, New J. Chem. 23 (1999) 1193–1196.
[31] C.C. Wong, W. Chu, Environ. Sci. Technol. 37 (2003) 2310–2316.
[32] G. Liu, J. Zhao, K. Wu, K. Oikawa, H. Hidaka, N. Serpone, Environ. Sci. Technol. 33 (1999) 2081–2087.
[33] G. Liu, X. Li, J. Zhao, H. Hidaka, N. Serpone, Environ. Sci. Technol. 34 (2000) 3982–3990.